A Quadrature Phase Detector in 28nm CMOS for Differential mm-Wave Sensing Applications using Dielectric Waveguides

Bart Philippe, Patrick Reynaert
KU Leuven, ESAT-MICAS
Kasteelpark Arenberg 10, 3001 Leuven, Belgium
Email: {bart.philippe, patrick.reynaert}@esat.kuleuven.be

***Abstract*—This paper presents a quadrature phase detector in 28nm CMOS, which is used to perform a differential phase measurement between two dielectric waveguides at 120 GHz. The phase detector has on-chip quadrature generation with a measured maximum quadrature error of 2° over a 20 GHz bandwidth. The quadrature phase detector achieves a maximum uncalibrated phase error of 11° . The proposed waveguide sensing system allows for both intrinsic measurements, in which the dielectric waveguide acts as a sensor, and extrinsic measurements, where the dielectric waveguide acts as a guided channel and antenna. Intrinsic sensing is demonstrated by a temperature measurement and extrinsic with a non-destructive test of a 3D-printed polymer sample.**

***Index Terms*—phase detector, quadrature, sensing, dielectric waveguide, mm-wave, CMOS**

I. Introduction

Technology scaling has advanced the RF-CMOS circuits in the mm-wave frequency range (30-300 GHz). This scaling has paved the way on the one hand for high speed communication applications and on the other hand for sensing applications. The sensing applications are driven by the increased resolution thanks to a decreased wavelength and transparency of dielectric materials. The most recent developments in the field of mm-wave sensing are based on radar sensors and permittivity measurements for blood sugar detection, cell characterization, and volume concentration measurement [1], [2]. These sensors measure permittivity by detecting a change in propagation or impedance of an on-chip microwave structure. This requires the dielectric material to be in close proximity to the chip. However, to apply mm-wave sensors into harsh or industrial environments, this paper proposes a differential phase measurement between two dielectric waveguides. The dielectric waveguides provide a low loss method to propagate the mm-waves between the chip and the measurement location. Furthermore a differential phase method reduces unwanted environmental interference on the measurement. The phase detection is performed by a quadrature phase detector in 28nm CMOS. The proposed receiver takes both the reference and measurement waveguide as input and provides a zero-IF quadrature output signal.

This receiver can enable multiple sensing applications from which we can distinguish two kinds. The first kind is an intrinsic measurement. In this measurement the guided wave does not leave the dielectric waveguide. The phase difference is caused by a change of propagation inside the waveguide due to the environment. The second kind is an extrinsic measurement, in this measurement the dielectric waveguide acts as a guided channel and antenna. The phase difference is caused by a change outside the waveguide. In this paper, intrinsic sensing is demonstrated by a temperature measurement and extrinsic with a non-destructive test (NDT) of a 3D-printed sample.

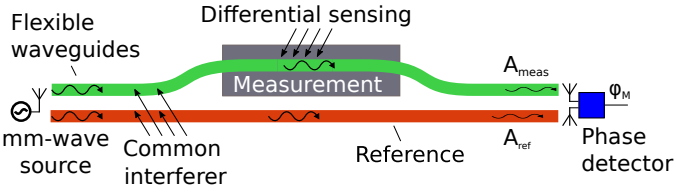

Fig. 1. System overview, differential phase sensing between 2 dielectric waveguides, rejecting unwanted common interference.

II. System Concept

The system, as shown in Fig. 1, consists of a mm-wave source coupling an EM-wave into two flexible, dielectric waveguides. One waveguide is used as a reference and the other for measurement, both are connected to the receiver. The mm-wave source couples an identical wave in both reference and measurement waveguide. Between the mm-wave source and the phase detector a common environmental change will impose an unwanted but identical phase shift and amplitude difference on both waveguides. To perform a measurement the waveguides diverge, and an amplitude difference α_M and phase difference ϕ_M, occurs between the measurement and reference waveguide. The receiver amplifies and downconverts both signals in quadrature to zero-IF resulting in the two base-band signals V_I and V_Q. Subsequently The phase information can be recovered by performing the inverse tangent of the ratio between V_I and V_Q, as shown in following equation:

$$\phi_M = arctan(\frac{V_I}{V_Q}) \tag{1}$$

The differential measurement mitigates the unwanted common phase interferers. Because of the quadrature output, the phase can be resolved without the knowledge of received signals

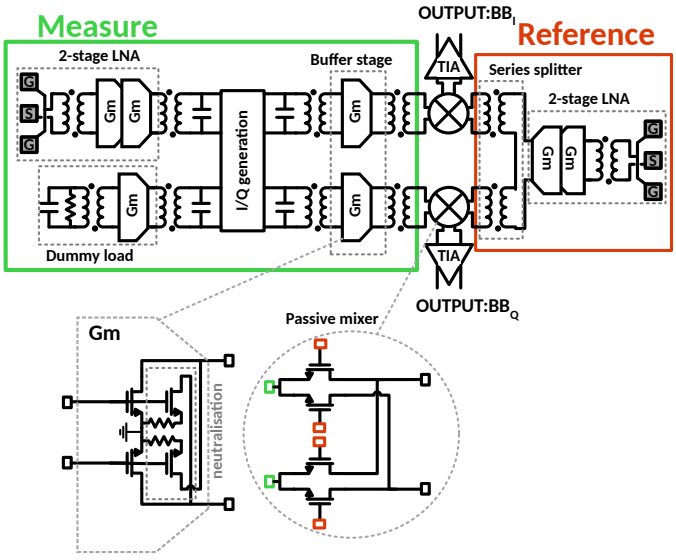

Fig. 2. Schematic of the quadrature phase detector.

magnitudes and is insensitive to unwanted amplitude interferers.

III. Phase Detector Design

Fig. 2 shows the proposed phase detector. Both reference and measurement inputs are first amplified by a two stage LNA. On one side I/Q generation is implemented as a differential $90°$ hybrid coupler followed by two buffer stages. Both sides are mixed together to zero-if by two passive current steering mixers and amplified by a TIA.

Both LNA's consist of two cascaded gain stages, implemented as as neutralized common-source stages, with a transformer based interstage matching network. The transistors of a single gain stage have 35 fingers with a finger width of $0.63\,\mu\mathrm{m}$. The neutralization is implemented as two dummy transistors to provide a well matched gate-drain capacitor. The input match is performed by a transmission line and a high-k, high-Q transformer. This results in a narrow band design. However, due to the low insertion-loss this also results in a better NF. The LNA, including input and output matching, has a simulated gain of $11\,\mathrm{dB}$.

On one side of the receiver the LNA is connected to the gates of the passive mixers with a series splitting transformer. On the other side the LNA is connected to the differential $90°$ hybrid coupler. The matching between the LNA stage and the coupler is made with a low coupled two-to-one transformer. A parallel plate capacitor is added at the $90°$ hybrid coupler side to tune out the transformer, the insertion loss is $2\,\mathrm{dB}$.

The phase error of the receiver is strongly dependent on the phase and amplitude imbalance between the I and Q channel. Therefore, a good quadrature generating structure is necessary. Generating quadrature at mm-wave frequencies with a traditional polyphase filter is very challenging due to layout parasitics. However, as the frequency increases transformer

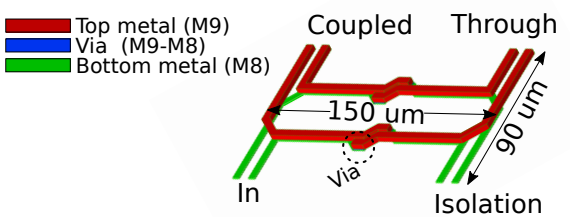

Fig. 3. Differential hybrid coupler implemented with two coupled lines between M9 and M8, symmetry is achieved by switching metal layer.

based hybrids or microwave structures can be implemented on-chip with a reasonable silicon area [3].

In this design, two coupled lines are combined to provide differential quadrature generation. This allows a differential design without the need of baluns. The structure is shown in Fig. 3. The coupler is fabricated in the two top metal layers with vertical coupling between the two metal layers. A symmetric design is achieved by switching metal layers in the middle of the coupler, resulting in an increased bandwidth. The coupler has a simulated phase error of $0.5°$ over the whole F-band for an area of $150\,\mu\mathrm{m} \times 90\,\mu\mathrm{m}$. The performance of the quadrature coupler is mainly determined by the matching between the coupler and the input LNA and output stages. The isolation port is connected to a dummy load to provide a matched impedance to the LNA stage at the input port. Phase tuning is possible by changing the gate-bias voltage of the dummy load. Both the coupled and the through port are matched to the input of a capacitive neutralized common-source stages with a one-to-two transformer and a capacitor at the coupler side to tune out the transformer's inductance. This stage provides an extra $9\,\mathrm{dB}$ gain and isolation between the passive mixer and the coupler. This isolation improves the quadrature performance by reducing the impedance change shown to the coupler by the passive mixer for high input powers.

Because of the zero-IF topology, a double balanced passive mixer is chosen to reduce dc-offset and 1/f noise. The sources of the passive mixers are matched to the drains of the gm stage with a two-to-one transformer to maximize the input current of the passive mixer [4]. The zero-IF current is amplified by a variable gain TIA to provide the two baseband signals V_I and V_Q.

IV. Measurement Results

A. Chip Characterisation

A die picture of the fabricated receiver in $28\,\mathrm{nm}$ bulk CMOS is shown in Fig. 4. The total area is $0.9\,\mathrm{mm}^2$ with an active RF area including GSG-pads of $0.37\,\mathrm{mm}^2$. The receiver consumes $103\,\mathrm{mW}$ from a $0.9\,\mathrm{V}$ supply. The input match and conversion gain measurements are performed using GSG-probes and shown in Fig. 5. The receiver has an input match below $-10\,\mathrm{dB}$ from $114\,\mathrm{GHz}$ to $134\,\mathrm{GHz}$. The quadrature performance for the whole chip is measured by transmitting 2-tones with a $1\,\mathrm{MHz}$ spacing. The measured phase and amplitude difference between the I and Q channel is shown

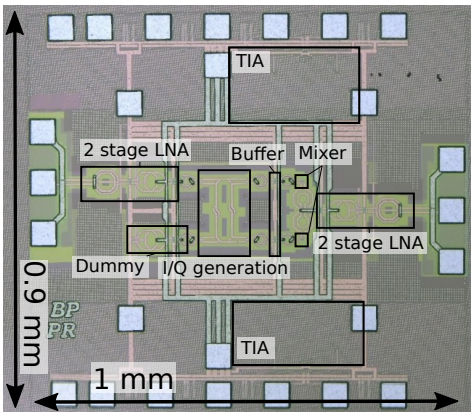

Fig. 4. Die photograph of the fabricated quadrature receiver in 28nm CMOS.

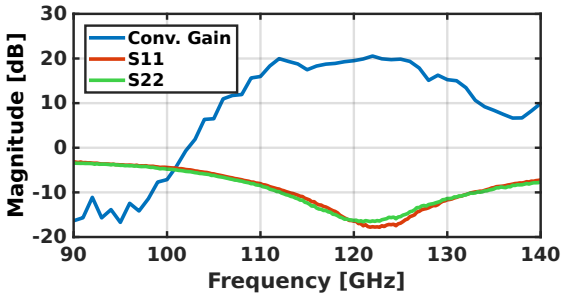

Fig. 5. Measured conversion gain for a reference input power of $-12\,\mathrm{dBm}$ and measured input match.

in Fig.6. The phase difference of the coupler can be tuned by changing the bias voltage of the dummy gm-stage, $0.65\,\mathrm{V}$ is the nominal tuning voltage. Over the bandwidth a maximum quadrature phase error of $2°$ and an amplitude imbalance of $-1.8\,\mathrm{dB}$ is measured. The phase demodulation measurement is performed by applying a phase shift using a calibrated WR-8 phaseshifter. Both I and Q channel are measured with a digital multimeter after which the voltages are applied to formula (1) to get the resulting phase. After removing a fixed phase offset the measurement is shown in Fig. 7. The maximum absolute uncalibrated phase error is $11°$ at $120\,\mathrm{GHz}$ and $9°$ at $125\,\mathrm{GHz}$.

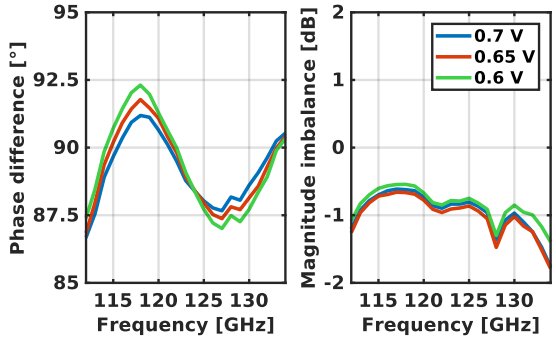

Fig. 6. Quadrature performance measurement for the receiver at low-IF by applying two tones with a $1\,\mathrm{MHz}$ spacing for 3 different dummy gate-bias voltages.

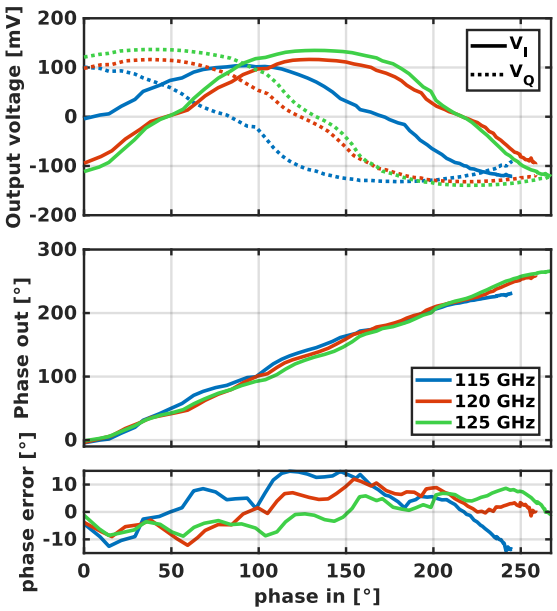

Fig. 7. Measured output voltage for a swept input phase (top), resulting demodulated phase using equation (1) with a phase offset compensation (middle) and the resulting phase error (bottom) for 115, 120 and $125\,\mathrm{GHz}$.

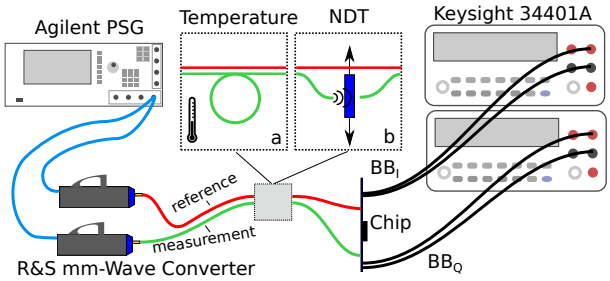

Fig. 8. The measurement setup for both application tests with, (a) the setup for a temperature measurement and (b) the setup for a NDT of a 3D-printed PLA sample.

B. Application Measurements

Two application measurements are performed. The measurement setup for both applications is shown in Fig. 8. The mm-wave source consists of two mm-wave converters connected to the same PSG, and generate $4\,\mathrm{dBm}$ output power at $120\,\mathrm{GHz}$. The mm-wave converters are coupled to the two dielectric waveguides with a circular horn antenna. In both case the dielectric waveguide is a circular PTFE fiber with a $2\,\mathrm{mm}$ diameter, surrounded by a $2\,\mathrm{mm}$ thick PTFE foam cladding. The two PTFE waveguides are coupled to the phase detector chip with a pcb using a circular horn-antenna which in turn is connected to a WR-8 waveguide to flip-chip transition.

The first measurement demonstrates intrinsic sensing with a temperature measurement. The mm-wave source and phase detector are connected with a reference waveguide of $1.8\,\mathrm{m}$ and a measurement waveguide of $4\,\mathrm{m}$. Both waveguides go through a temperature controlled chamber, a 1.9m length difference results in a measurable phase difference with temperature. The

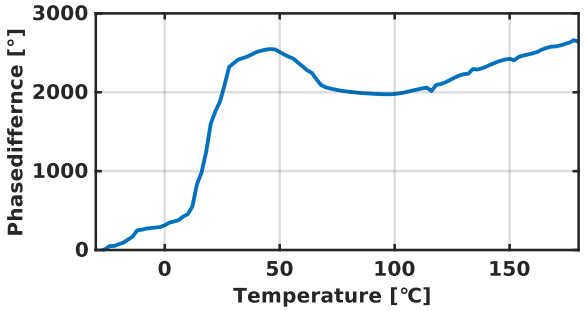

Fig. 9. Measured unwrapped output phase for a temperature sweep from -30° to 180° C with a 2° step at 130 GHz.

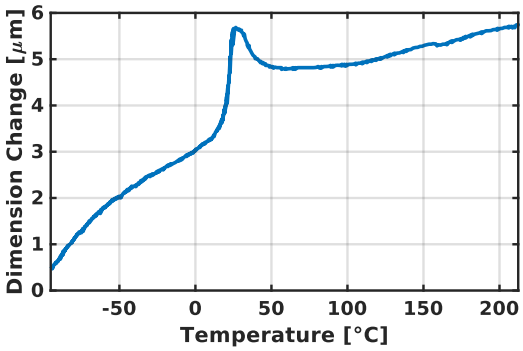

Fig. 10. Thermal expansion of PTFE as comparison [6]

temperature is swept from -30° to 180° C with a 2° step, the unwrapped output phase is shown in Fig. 9. A correlation between the measured phase and the the non-linear thermal expansion of PTFE [5], as shown in Fig. 10 [6], is visible . The thermal expansion of PTFE is dependent on the fabrication and crystallization of the PTFE material. This provides a method to characterize the phase response of a PTFE fiber versus temperature.

The second measurement demonstrates extrinsic sensing by performing a NDT to ensure material integrity. A difference in dielectric constant between an air void and filled material results in a measurable phase difference which enables the detection of hidden voids in a polymer sample. The first mm-wave source is connected to the receiver through a 70 cm long circular PTFE reference waveguide. A second waveguide is cut in half and connects the second mm-wave source to the receiver. An air gap of 4 cm separates the two halves. The measurement is performed by moving the sample under test (SUT) between the air gap using a mechanical stepper with a unit-step of 50 µm. The SUT is a 3D-printed PLA box of 3 mm thick with hidden internal air voids of 1 mm high, thus providing a change in dielectric constant. The measurement result is shown in Fig. 11. The top figure shows the measured phase change. The bottom figure depicts the 3D print including voids. The air voids show a 90° phase difference compared to the filled PLA. The smallest detected void has a width of 620 µm or 0.25λ. The detected voids show a consistent phase difference and the width of each void shows a good

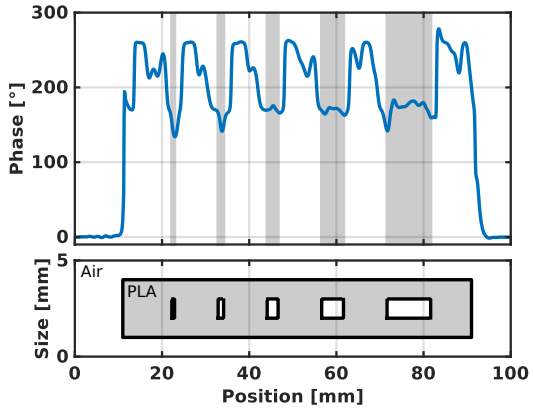

Fig. 11. A non-destructive test of a 3D-printed structure in PLA at 120 GHz. The top figure shows the measured phase. The bottom figure represents the internal structure of the 3D-print.

correspondence to the actual size.

V. Conclusion

A quadrature receiver in 28nm CMOS for differential phase measurement at 120 GHz, enabling industrial differential mm-wave sensing applications using dielectric waveguides is demonstrated. The receiver has on-chip quadrature generation with a measured maximum quadrature error of 2° over the complete bandwidth. The receiver achieves a maximum uncalibrated phase error of 9° at 125 GHz. Both intrinsic and extrinsic sensing examples are shown. The first example uses the dielectric waveguide to perform a temperature measurement from -30° to 180° C and shows a phase difference of 2640° at 130 GHz. The second example uses the dielectric waveguide as a guided channel and antenna to perform a non-destructive test on a plastic 3D print a phase shift of 90° is measured for a 1 mm void height and the smallest detected void has a width of 620 µm or 0.25λ. These experiments show the applicability of CMOS and dielectric waveguides for various sensing applications.

References

[1] J. Wessel, K. Schmalz, J. C. Scheytt, and D. Kissinger, "A 120-GHz Electrical Interferometer for Contactless Permittivity Measurements with Direct Digital Read-Out," *IEEE Microwave and Wireless Components Letters*, vol. 27, no. 2, pp. 198–200, 2017.

[2] B. Laemmle, K. Schmalz, J. C. Scheytt, R. Weigel, and D. Kissinger, "A 125-GHz permittivity sensor with read-out circuit in a 250-nm SiGe BiCMOS technology," *IEEE Transactions on Microwave Theory and Techniques*, vol. 61, no. 5, pp. 2185–2194, 2013.

[3] A. Medra, D. Guermandi, K. Vaesen, S. Brebels, A. Bourdoux, W. Van Thillo, P. Wambacq, and V. Giannini, "An 80 GHz Low-Noise Amplifier Resilient to the TX Spillover in Phase-Modulated Continuous-Wave Radars," *IEEE J. Solid-State Circuits*, vol. 51, no. 5, pp. 1141–1153, 2016.

[4] C. H. Li, Y. L. Liu, and C. N. Kuo, "A 0.6-V 0.33-mW 5.5-GHz receiver front-end using resonator coupling technique," *IEEE Transactions on Microwave Theory and Techniques*, vol. 59, no. 6, pp. 1629–1638, 2011.

[5] M. M. S. C. Blumm J., Lindemann A., "Characterization of ptfe using advanced thermal analysis techniques," *International Journal of Thermophysics*, vol. 31, no. 10, pp. 1919–1927, Oct 2010.

[6] (2018) Thermal expansion of ptfe crystalline phase. [Online]. Available: http://www.andersonmaterials.com/cte-thermal-expansion.html